RNA editing controls meiotic drive by a Neurospora Spore killer

Nicholas A. Rhoades and Thomas M. Hammond[1]

School of Biological Sciences, Illinois State University, Normal, Illinois 61790

[1]Corresponding author

Thomas M. Hammond

School of Biological Sciences

Illinois State University

Normal, IL 61790

Phone: 309-438-2602

Email: tmhammo@ilstu.edu

Running title

RNA editing controls spore killing

KEYWORDS

fungi, gene driver, meiotic drive, RNA editing, spore killing

ABSTRACT

Neurospora *Sk-2* is a complex meiotic drive element that is transmitted to offspring through sexual reproduction in a biased manner. *Sk-2*'s biased transmission mechanism involves spore killing, and recent evidence has demonstrated that spore killing is triggered by a gene called *rfk-1*. However, a second gene, *rsk*, is also critically important for meiotic drive by spore killing because it allows offspring with an *Sk-2* genotype to survive the toxic effects of *rfk-1*. Here, we present evidence demonstrating that *rfk-1* encodes two protein variants: a 102 amino acid RFK-1^{A} and a 130 amino acid RFK-1^{B}, but only RFK-1^{B} is toxic. We also show that expression of RFK-1^{B} requires an early stop codon in *rfk-1* mRNA to undergo adenosine-to-inosine (A-to-I) mRNA editing. Finally, we demonstrate that RFK-1^{B} is toxic when expressed within vegetative tissue of Spore killer sensitive (Sk^{S}) strains, and that this vegetative toxicity can be overcome by co-expressing *Sk-2*'s version of RSK. Overall, our results demonstrate that *Sk-2* uses RNA editing to control when its spore killer is produced, and that the primary killing and resistance functions of *Sk-2* can be conferred upon an Sk^{S} strain by the transfer of only two genes.

INTRODUCTION

Neurospora *Spore killer-2* (*Sk-2*) is a complex meiotic drive element with the ability to be transmitted to nearly all viable offspring produced by sexual reproduction (Turner and Perkins 1979). While *Sk-2*'s biased transmission rate is caused by spore killing, the molecular processes directing the mechanism of spore killing are unclear. We have previously demonstrated that spore killing requires at least two proteins: RFK-1 (Required For Killing-1) and RSK (Resistant to Spore Killer) (Hammond *et al.* 2012; Harvey *et al.* 2014; Rhoades *et al.* 2019). It is currently thought that RFK-1 provides the killing function, and that RSK provides the resistance function;

however, *Sk-2* is a complex meiotic drive element that spans more than 2.5 Mb of chromosome III and it includes hundreds of linked protein-coding genes (Svedberg *et al.* 2018). Therefore, it is possible that *Sk-2* possesses other genes that are required for either killing, resistance, or both. We sought to test this hypothesis by genetically engineering a non-*Sk-2* strain (Sk^S; Spore killer sensitive) to carry copies of *Sk-2*'s *rfk-1* and *rsk* alleles, referred to as $rfk\text{-}1^{Sk\text{-}2}$ and $rsk^{Sk\text{-}2}$, respectively. As part of this process, we examined the role of a previously identified nucleotide within $rfk\text{-}1^{Sk\text{-}2}$ mRNAs that undergoes adenosine-to-inosine (A-to-I) mRNA editing in Sk^S × *Sk-2* crosses.

MATERIALS AND METHODS

Strains and media

The genotypes of all strains used in this study are listed in Table 1. Vogel's Minimal Medium (VMM) or Vogel's Minimal Agar (VMA: VMM + 2% agar) (Vogel 1956) was used for vegetative propagation of all Neurospora strains unless otherwise indicated. L-histidine (Research Products International) was added to growth medium at 0.5 g per liter for propagation of strains with a *his-3* mutation. Hygromycin B (Gold Biotechnology) was used at 200 µg per ml when selecting for hygromycin resistant strains. Westergaard and Mitchell's synthetic crossing agar (SCA) (Westergaard and Mitchell 1947) with 1.5% sucrose and a pH of 6.5 was used for *N. crassa* crosses. Brockman and de Serres agar (BDA) (Brockman and De Serres 1963) with 1% sorbose, 0.05% glucose, 0.05% fructose, 2.0% agar, and the recommended salts + minerals was used to select homokaryotic strains from heterokaryotic transformants. The $mus\text{-}51^{RIP70}$ allele is available in strain FGSC 10340 from the Fungal Genetics Stock Center (McCluskey *et al.* 2010).

Plasmid construction and site directed mutagenesis

AH36 is a 1481 bp *rfk-1*-spanning interval of *Sk-2* DNA (Rhoades *et al.* 2019) (GenBank KJ908288.1: positions 27900–29380). Plasmid pNR9.1 was constructed by amplifying AH36 from *Sk-2* genomic DNA with primer set 353/639 and cloning the PCR product between the *Not*I sites of plasmid pBluescript II KS(-) (the sequences of the primers used in this study are listed in Table S1).

Plasmid pNR127.9 was constructed by changing the first *rfk-1* stop codon in pNR9.1 from TAG to TGG with primer set 1727/1728 and the Q5 Site-Directed Mutagenesis Kit (New England Biolabs). Similarly, plasmid pNR153.1 was constructed by changing the first *rfk-1* stop codon in pNR9.1 from TAG to TAA with primer set 1789/1791 and the Q5 Site-Directed Mutagenesis Kit.

Plasmids pNR154.4 and pNR154.6 were constructed by transferring a 1.5 kb *Not*I fragment containing $rfk\text{-}1^{Sk\text{-}2}$ from pNR9.1 to the *Not*I site of pTH1256.1 (GenBank, MH550659.1). The $rfk\text{-}1^{Sk\text{-}2}$ and *hph* coding sequences are in opposite orientations in pNR154.4 and identical orientations in pNR154.6, respectively. Plasmid pNR155.2 was constructed by transferring the 1.5 kb *Not*I fragment containing $rfk\text{-}1^{TAG>TGG}$ from pNR127.9 to the *Not*I site of pTH1256.1 and selecting for the *rfk-1* transcriptional direction that matched that of *hph* within pTH1256.1. Plasmid pNR157.6 was constructed by transferring a 1.5 kb *Not*I fragment containing $rfk\text{-}1^{TAG>TAA}$ from pNR153.1 to the *Not*I site of pTH1256.1, and selecting for an *rfk-1* transcriptional direction that was opposite to that of *hph* within pTH1256.1.

DJ-PCR product construction

DJ-PCR products were produced with Q5® High-Fidelity DNA Polymerase (New England Biolabs) via the method of Yu *et al.* (2004). DJ-PCR product v251a was constructed to fuse the coding region of *rfk-1*$^{TAG>TGG}$ to the *tcu-1* promoter on chromosome I of an *Sk*^{S} strain while deleting the coding sequences of *tcu-1* (the sequences of the *tcu-1* locus and other non-*Sk-2*-specific loci were downloaded from FungiDB [Stajich *et al.* 2012]). The left and right flanks for DJ-PCR were amplified from wildtype genomic DNA with primer sets 1845/1846 and 1847/1848, respectively. The center fragment for DJ-PCR was amplified from pNR155.2 with primer set 1843/1844. The fused DJ-PCR product was amplified with primer set 1849/1850 for use in *N. crassa* transformation. DJ-PCR product v251b was constructed to fuse the coding region of *rfk-1*$^{Sk-2}$ to the *tcu-1* promoter on chromosome I in an *Sk*^{S} strain while deleting the coding sequences of *tcu-1*. It was constructed similarly to v251a except that the center fragment was amplified from pNR154.6.

DJ-PCR product v286 was constructed to insert *hph* downstream of the *rsk*$^{Sk-2}$ gene on chromosome III in an *Sk-2* strain (Figure S1). The left and right flanks were amplified from genomic DNA of *Sk-2* strain P15-53 with primer sets 1985/1986 and 1987/1988, respectively. The center fragment was amplified from plasmid pTH1256.1 with primer set 12/13. The fused DJ-PCR product was amplified with primer set 1989/1990 for use in *N. crassa* transformation.

DJ-PCR product v290 was constructed to fuse the coding region of *rfk-1*$^{Sk-2}$ to the *ccg-1* promoter (McNally and Free 1988) on chromosome V of an *Sk*^{S} strain while deleting the *ccg-1* coding sequences. The left and right flanks were amplified from wildtype genomic DNA with

primer sets 2011/2012 and 2013/2014, respectively. The center fragment was amplified from genomic DNA of strain TNR278.1 with primer set 2015/2016. The fused DJ-PCR product was amplified with primer set 2015/2016 for use in *N. crassa* transformation.

N. crassa transformations

Transformation of *N. crassa* was performed by the electroporation method of Margolin *et al.* (1997) with modifications as described by Rhoades *et al.* (2020). Strains ISU-4954 and ISU-4955 were obtained by transformation of strain P8-43 with plasmids pNR154.4 and pNR157.6, respectively. Histidine prototrophy and hygromycin B resistance were used to select transformants. Homokaryotic transformants were obtained from heterokaryons through microconidia purification (Ebbole and Sachs 1990) and confirmed by PCR.

Strains ISU-4956 and ISU-4957 were obtained by transformation of FGSC 10340 with DJ-PCR products v251a and v251b, respectively. For these transformations, $CuSO_4$ was included in the transformation media at 250 µM. Homokaryotic transformants were obtained by single conidium isolation. The single conidium isolation procedure involved spreading dilute conidial suspensions onto BDA + 250 µM $CuSO_4$ and, after approximately 16 hours of incubation at 32 °C and 24 hours at room temperature, transferring germlings to VMA + 250 $CuSO_4$ slants with the aid of a dissecting microscope. Homokaryons were then distinguished from heterokaryons by PCR.

Strain ISU-4958 was obtained by transformation of P15-53 with DJ-PCR product v286. Hygromycin B was used to select transformants. Strain ISU-4959 was obtained by

transformation of strain FGSC 10340 with DJ-PCR product v290. Transformants were selected on medium containing hygromycin B.

Growth assays

Radial growth assays were performed in 100 mm culture dishes containing VMA or VMA + 250 µM $CuSO_4$. A 5 µl aliquot of a 1000 conidia per µl suspension (made in sterile water) was transferred to the center of each dish. Inoculated plates were imaged after 120 h of growth at room temperature. Linear growth assays were performed in 25 ml polystyrene serological pipettes (Corning™ 4489) according to the method of White and Woodward (1995). The pipettes were inoculated with 5 µl aliquots of a 1000 conidia per µl suspension (made in sterile water) and growth front positions were recorded at 24-hour intervals.

Spore killing assays

Unidirectional crosses were performed on SCA as previously described (Samarajeewa *et al.* 2014). Asci (ascospore sacs) were dissected from fruiting bodies into 50% glycerol on the 14th day after fertilization. Digital images of asci (ascospore sacs) were obtained with the aid of a Leica DMBRE microscope and imaging system.

RESULTS

A-to-I mRNA editing is required for spore killing

In a previous report, we demonstrated that *rfk-1*$^{Sk-2}$ undergoes A-to-I mRNA editing (herein referred to as RNA editing) of an early stop codon during the sexual phase (Rhoades *et al.* 2019). With the sequence of *rfk-1*$^{Sk-2}$, the position of the edited stop codon, and the standard rules of

mRNA translation, we predicted that *rfk-1*$^{Sk\text{-}2}$ encodes at least two protein variants: a shorter protein of 102 amino acids and a longer protein of 130 amino acids (Figure 1A; Rhoades *et al.* 2019). Here, we refer to the shorter variant as RFK-1^{A} and the longer variant as RFK-1^{B}.

We have also shown that a 1481 bp *rfk-1*$^{Sk\text{-}2}$-spanning interval of *Sk-2* DNA called AH36 (Figure S2) can be placed downstream of the *his-3* locus in an *Sk*^{S} strain without overtly influencing vegetative growth and vegetative developmental processes (Rhoades *et al.* 2019). However, if an AH36-harboring strain is crossed with an *Sk*^{S} mating partner, ascus development is aborted before the formation of viable ascospores. This ascus abortion phenotype is consistent with the presence of *Sk-2*'s killer and the concomitant absence of *Sk-2*'s resistance protein during ascus development, and because it occurs when *rfk-1*$^{Sk\text{-}2}$ is present, it suggests that at least one RFK-1 variant is required for the ascus abortion phenotype.

To determine if RFK-1^{A}, RFK-1^{B}, or both are required for the ascus abortion phenotype, we inserted a modified AH36 downstream of the *his-3* locus on chromosome I in an *Sk*^{S} strain (Figure 2A). The modified AH36 includes *rfk-1*$^{TAG>TAA}$ instead of *rfk-1*$^{Sk\text{-}2}$. The *rfk-1*$^{TAG>TAA}$ sequence is identical to *rfk-1*$^{Sk\text{-}2}$ except that its early stop codon has been changed to TAA. We predicted that if RNA editing of the early stop codon in *rfk-1*$^{TAG>TAA}$ were to occur, it would produce a TGA (i.e., UGA) stop codon. Thus, *rfk-1*$^{TAG>TAA}$ should express RFK-1^{A} but not RFK-1^{B}. As a control, we reinserted an unmodified AH36 containing *rfk-1*$^{Sk\text{-}2}$ downstream of the *his-3* locus in an *Sk*^{S} strain, thereby repeating the original experiment performed by Rhoades *et al.* (2019).

Interestingly, we found that expression of *rkf-1*$^{TAG>TAA}$ within AH36 during meiosis has no apparent effect on ascus development when both parents are of the *Sk*^{S} genetic background, while, consistent with previous results, expression of *rkf-1*$^{Sk-2}$ within AH36 under the same conditions causes ascus abortion (Figure 2, B–E). These results demonstrate that RNA editing of the early stop codon in *rfk-1*$^{Sk-2}$ from TAG to TGG (i.e., UAG to UGG) is required for expression of RFK-1^{B} and that RFK-1^{B} expression is required for the ascus abortion phenotype.

RFK-1^{B} but not RFK-1^{A} is toxic to vegetative tissue

While the above results demonstrate that RFK-1^{B} is required for the ascus abortion phenotype, they do not address the role of RFK-1^{A} in ascus abortion. For example, perhaps RFK-1^{A} and RFK-1^{B} must both be present within an ascus for ascus abortion to occur. We tried to test this hypothesis by inserting an *rfk-1*$^{TAG>TGG}$-containing AH36 downstream of the *his-3* locus in an *Sk*^{S} strain. The *rfk-1*$^{TAG>TGG}$ sequence is identical to *rfk-1*$^{Sk-2}$ except that the early TAG stop codon has been changed to TGG. As a result, *rfk-1*$^{TAG>TGG}$ should express RFK-1^{B} but not RFK-1^{A}. However, our attempts to insert an *rfk-1*$^{TAG>TGG}$-containing AH36 downstream of the *his-3* locus in an *Sk*^{S} strain failed to produce a successful transformant (data not shown).

Our inability to recover a transformant carrying an *rfk-1*$^{TAG>TGG}$-containing AH36 downstream of the *his-3* locus in an *Sk*^{S} genetic background suggested that *rfk-1*$^{TAG>TGG}$ is toxic to *Sk*^{S} strains. To test this hypothesis, we inserted the coding region of *rfk-1*$^{TAG>TGG}$ immediately downstream of the copper repressible *tcu-1* promoter on chromosome I while suppressing expression of *rfk-1*$^{TAG>TGG}$ with 250 μM of $CuSO_4$ (Figure 3A; Lamb *et al.* 2013). As a control, we also inserted the coding region of *rfk-1*$^{Sk-2}$ immediately downstream of the *tcu-1* promoter.

We then compared the vegetative growth characteristics of strains carrying either *tcu-1(P)-rfk-1*$^{Sk\text{-}2}$ or *tcu-1(P)-rfk-1*$^{TAG>TGG}$ on low copper (inducing) and high copper (repressing) media. Interestingly, while the *tcu-1(P)-rfk-1*$^{Sk\text{-}2}$ strain grew similarly on low and high copper media, the *tcu-1(P)-rfk-1*$^{TAG>TGG}$ strain grew poorly under low copper conditions and normally under high copper conditions (Figure 3, B and C; Table 2). These results demonstrate that RFK-1^{B} can exert its toxic effects on vegetative tissue. They also demonstrate that RFK-1^{A} is not required for the toxicity of RFK-1^{B} in vegetative tissue.

RSK$^{Sk\text{-}2}$ neutralizes RFK-1^{B} toxicity in vegetative tissue

To determine if RSK$^{Sk\text{-}2}$ can neutralize RFK-1^{B}'s toxicity in vegetative tissue, we inserted the coding region of *rsk*$^{Sk\text{-}2}$ downstream of the high expression *ccg-1* promoter on chromosome V in an *Sk*^{S} strain (Figure 4A). We then combined the *ccg-1(P)-rsk*$^{Sk\text{-}2}$ and *tcu-1(P)-rfk-1*$^{TAG>TGG}$ alleles in a single strain through a sexual cross, and analyzed the resulting strain's growth characteristics on low and high copper media. Interestingly, we found there to be little difference in the strain's vegetative morphology or linear growth rate under low and high copper conditions (Figure 4, B and C; Table 2). These observations contrast with those made of strain ISU-4956, which possesses *tcu-1(P)-rfk-1*$^{TAG>TGG}$ but not *ccg-1(P)-rsk*$^{Sk\text{-}2}$ (Figure 3, B and C; Table 2). These findings demonstrate that RSK$^{Sk\text{-}2}$ neutralizes the toxicity of RFK-1^{B} in vegetative tissue.

DISCUSSION

In this study, we have provided evidence that RNA editing (specifically, A-to-I mRNA editing) of an early stop codon in *rfk-1*$^{Sk\text{-}2}$ is necessary for spore killing. We have also shown that RFK-1^{B}, one of two RFK-1 variants, is toxic to vegetative tissue. Finally, we have shown that

RSK$^{Sk\text{-}2}$ neutralizes RFK-1^{B} in vegetative tissue. These results are consistent with the killer neutralization (KN) model of *Sk-2* meiotic drive (Hammond *et al.* 2012).

The KN model holds that *Sk-2*'s killer protein is neutralized by *Sk-2*'s resistance protein during early stages of ascus development. At later stages of development, likely after ascospore delimitation, the resistance protein becomes restricted to ascospores that inherit *Sk-2* (i.e., *Sk-2* ascospores). Ascospores that do not inherit *Sk-2*, such as the Sk^{S} ascospores of an *Sk-2* × Sk^{S} cross, succumb to the killer's toxic effects because they cannot produce the resistance protein. If the KN model is accurate, the killer should have a half-life that is longer than that of the resistance protein, or the killer should be able to move from *Sk-2* ascospores to Sk^{S} ascospores after ascospore delimitation.

Although it had previously been shown that the early stop codon in *rfk-1*$^{Sk\text{-}2}$ mRNAs is edited from UAG to UGG during the sexual phase, the role of this edit in spore killing was not investigated (Rhoades *et al.* 2019). Here, we have shown that editing of the early stop codon in *rfk-1*$^{Sk\text{-}2}$ mRNAs allows for expression of RFK-1^{B}. We have also shown that alleles which cannot express RFK-1^{B}, such as *rfk-1*$^{TAG>TAA}$, do not trigger the ascus abortion phenotype (Figure 2E), which occurs when the *Sk-2* killer is expressed without co-expression of a compatible resistance protein (Rhoades *et al.* 2019). The most likely explanation for why *rfk-1*$^{TAG>TAA}$ does not trigger ascus abortion is that its TAG to TAA mutation prevents RNA editing from changing the resulting early UAA stop codon to UGG, a tryptophan codon. If RNA editing does occur, we expect that it would change the early UAA stop codon in *rfk-1*$^{TAG>TAA}$ mRNAs to UGA, which is

also a stop codon. Therefore, it is likely that *rfk-1*$^{TAG>TAA}$ mRNAs can only be used by ribosomes to produce RFK-1^{A}.

Our study of *rfk-1*$^{Sk\text{-}2}$ suggests that it encodes at least two protein variants: the 102 aa RFK-1^{A} and the 130 aa RFK-1^{B}. Furthermore, our results support a model in which RFK-1^{A} is non-toxic and RFK-1^{B} is toxic. We have presented two lines of evidence for the non-toxicity of RFK-1^{A}: first, the RFK-1^{A}-specific *rfk-1*$^{TAG>TAA}$ allele does not trigger ascus abortion in *Sk*^{S} *sad-2*$^{\Delta}$ × *rfk-1*$^{TAG>TAA}$ crosses (Figure 2E), demonstrating that expression of RFK-1^{A} alone during ascus development is not harmful; and second, expression of *rfk-1*$^{Sk\text{-}2}$ during the vegetative phase does not reduce growth rate or overtly influence vegetative morphology. This latter finding is relevant to the non-toxicity of RFK-1^{A} because A-to-I mRNA editing does not occur during the vegetative phase in *N. crassa* (Liu *et al.* 2017), and thus translation of *rfk-1*$^{Sk\text{-}2}$ mRNAs during the vegetative phase should produce RFK-1^{A} but not RFK-1^{B}. We have also presented two lines of evidence for the toxicity of RFK-1^{B}. First, ascus abortion occurs during *Sk*^{S} *sad-2*$^{\Delta}$ × *rfk-1*$^{Sk\text{-}2}$ crosses but not during *Sk*^{S} *sad-2*$^{\Delta}$ × *rfk-1*$^{TAG>TAA}$ crosses (Figure 2, D and E), and RFK-1^{B} should only be expressed in the former cross type; and second, expression of the RFK-1^{B}-specific *rfk-1*$^{TAG>TGG}$ allele during the vegetative phase significantly restricts vegetative growth (Figure 3, B and C; Table 2).

The KN model holds that the *Sk-2* killer is neutralized by the *Sk-2* resistance protein. Our results strongly suggest that the *Sk-2* killer is RFK-1^{B} and that RFK-1^{B} is neutralized by RSK$^{Sk\text{-}2}$. Furthermore, our results suggest that a second *Sk-2* specific gene product is not required for either the toxicity of RFK-1^{B} or the resistance properties of RSK$^{Sk\text{-}2}$. For example, although

expression of RFK-1^{B} in vegetative tissue is toxic in an *Sk*^{S} genetic background (Figure 3, B and C; Table 2), this toxicity can be overcome by co-expression of RSK^{Sk-2} (Figure 4, B and C; Table 2). Still, *Sk-2* is a complex meiotic drive element containing hundreds of linked protein coding genes (Svedberg *et al.* 2018), and it remains possible that some of these *Sk-2*-linked genes modify the efficiency of the spore killing and/or resistance processes. Testing this hypothesis will likely require construction of a functional two-gene meiotic drive element containing only *rsk*$^{Sk-2}$ and *rfk-1*$^{Sk-2}$ and comparing the efficiency of meiotic drive by *Sk-2* with that of the two gene element.

ACKNOWLEDGEMENTS

We would like to thank members of the Hammond Laboratory at ISU for technical assistance with this work. This work was supported by awards to TMH from the National Science Foundation (1615626 / 2005295).

LITERATURE CITED

Brockman H. E., and F. J. De Serres, 1963 “Sorbose toxicity” in Neurospora. Am. J. Bot. 50: 709–714. https://doi.org/10.2307/2440049

Ebbole D., and M. Sachs, 1990 A rapid and simple method for isolation of *Neurospora crassa* homokaryons using microconidia. Fungal Genet. Newsl. 37: 17–18.

Hammond T. M., D. G. Rehard, H. Xiao, and P. K. T. Shiu, 2012 Molecular dissection of the *Neurospora crassa* Spore killer elements. Proc. Natl. Acad. Sci. U. S. A. in press.

Hammond T. M., 2017 Sixteen years of meiotic silencing by unpaired DNA. Adv. Genet. 97: 1–42. https://doi.org/10.1016/bs.adgen.2016.11.001

Harvey A. M., D. G. Rehard, K. M. Groskreutz, D. R. Kuntz, K. J. Sharp, *et al.*, 2014 A critical component of meiotic drive in Neurospora is located near a chromosome rearrangement. Genetics. https://doi.org/10.1534/genetics.114.167007

Lamb T. M., J. Vickery, and D. Bell-Pedersen, 2013 Regulation of gene expression in *Neurospora crassa* with a copper responsive promoter. G3 3: 2273–2280. https://doi.org/10.1534/g3.113.008821

Liu H., Y. Li, D. Chen, Z. Qi, Q. Wang, *et al.*, 2017 A-to-I RNA editing is developmentally regulated and generally adaptive for sexual reproduction in *Neurospora crassa*. Proc. Natl. Acad. Sci. U. S. A. 114: E7756–E7765. https://doi.org/10.1073/pnas.1702591114

Margolin B. S., M. Freitag, and E. U. Selker, 1997 Improved plasmids for gene targeting at the *his-3* locus of *Neurospora crassa* by electroporation. Fungal Genet. Newsl. 44: 34–36.

McCluskey K., A. Wiest, and M. Plamann, 2010 The Fungal Genetics Stock Center: a repository for 50 years of fungal genetics research. J. Biosci. 35: 119–126.

McNally M. T., and S. J. Free, 1988 Isolation and characterization of a Neurospora glucose-repressible gene. Curr. Genet. 14: 545–551. https://doi.org/10.1007/BF00434079

Rhoades N. A., A. M. Harvey, D. A. Samarajeewa, J. Svedberg, A. Yusifov, *et al.*, 2019 Identification of *rfk-1*, a meiotic driver undergoing RNA editing in Neurospora. Genetics 212: 93–110. https://doi.org/10.1534/genetics.119.302122

Rhoades N. A., E. K. Webber, and T. M. Hammond, 2020 A nonhomologous end-joining mutant for *Neurospora sitophila* research. Fungal Genet. Rep. 64: Article 1. https://doi.org/10.4148/1941-4765.2172

Samarajeewa D. A., P. A. Sauls, K. J. Sharp, Z. J. Smith, H. Xiao, *et al.*, 2014 Efficient detection of unpaired DNA requires a member of the Rad54-like family of homologous recombination proteins. Genetics 198: 895–904. https://doi.org/10.1534/genetics.114.168187

Shiu P. K. T., D. Zickler, N. B. Raju, G. Ruprich-Robert, and R. L. Metzenberg, 2006 SAD-2 is required for meiotic silencing by unpaired DNA and perinuclear localization of SAD-1 RNA-directed RNA polymerase. Proc. Natl. Acad. Sci. U. S. A. 103: 2243–2248. https://doi.org/10.1073/pnas.0508896103

Stajich J. E., T. Harris, B. P. Brunk, J. Brestelli, S. Fischer, *et al.*, 2012 FungiDB: an integrated functional genomics database for fungi. Nucleic Acids Res. 40: D675-681. https://doi.org/10.1093/nar/gkr918

Svedberg J., S. Hosseini, J. Chen, A. A. Vogan, I. Mozgova, *et al.*, 2018 Convergent evolution of complex genomic rearrangements in two fungal meiotic drive elements. Nat. Commun. 9: 4242. https://doi.org/10.1038/s41467-018-06562-x

Turner B. C., and D. D. Perkins, 1979 Spore killer, a chromosomal factor in neurospora that kills meiotic products not containing it. Genetics 93: 587–606.

Vogel H. J., 1956 A convenient growth medium for Neurospora (Medium N). Microb. Genet Bull 13: 42–43.

Westergaard M., and H. K. Mitchell, 1947 Neurospora V. A synthetic medium favoring sexual reproduction. Am. J. Bot. 34: 573–577. https://doi.org/10.2307/2437339

White B., and D. Woodward, 1995 A simple method for making disposable race tubes. Fungal Genet. Rep. 42: Article 27.

Yu J.-H., Z. Hamari, K.-H. Han, J.-A. Seo, Y. Reyes-Domínguez, *et al.*, 2004 Double-joint PCR: a PCR-based molecular tool for gene manipulations in filamentous fungi. Fungal Genet. Biol. FG B 41: 973–981. https://doi.org/10.1016/j.fgb.2004.08.001

FIGURE LEGENDS

Figure 1 Predicted sequences of RFK-1^{A} and RFK-1^{B}. RFK-1^{A} contains 102 amino acids. RFK-1^{B} contains 130 amino acids. The first 102 amino acids in RFK-1^{B} are identical to those in RFK-1^{A}. The underlined sequence is unique to RFK-1^{B}.

Figure 2 A-to-I RNA editing controls RFK-1 toxicity. **(**A) The *N. crassa his-3* locus on chromosome I is illustrated at the top of the diagram. The position of the *his-3* coding sequence is depicted with a white rectangle, as is the coding sequence for gene *ncu03140*. The directions of transcription are indicated with black arrows. Intron positions within coding sequences are not indicated. The diagram was drawn to scale and the orange bar represents the 919 bp of intergenic sequence that was deleted and replaced with *rfk-1*/AH36 sequences and a selectable marker (*hph*). The red asterisks represent the approximate positions of the two *rfk-1* stop codons. (B–D) In Neurospora fungi, meiosis and ascospore development occurs in cells called asci. Asci from the following crosses are shown: (B) F2-26 × ISU-4954, (C) F2-26 × ISU-4955, (D) ISU-3037 × ISU-4954, and (E) ISU-3037 × ISU-4955. Note that suppression of meiotic silencing by unpaired DNA (MSUD) with the *sad-*2^{Δ} allele is needed to express unpaired genes, such as *rfk-*$1^{Sk\text{-}2}$ and *rfk-*$1^{TAG>TAA}$ in the above crosses, during meiosis (Shiu *et al.* 2006; Hammond 2017; Rhoades *et al.* 2019).

Figure 3 RFK-1^{B} expression restricts vegetative growth. **(**A) The relative positions of *N. crassa* genes *ncu00829*, *tcu-1*, and *ncu00831* on chromosome I are illustrated at the top the panel. Coding sequences are depicted as white rectangles. Intron positions are not indicated. The diagram was drawn to scale and the orange bar represents the 936 bp of DNA that were deleted

and replaced with *rfk-1* sequences and a selectable marker (*hph*). The red asterisks represent the approximate positions of the two *rfk-1* stop codons. (B) Images of *N. crassa* cultures after five days of growth. Conidial suspensions were inoculated to the center of 100 mm culture dishes containing VMA or VMA + 250 µM $CuSO_4$. (C) Linear growth on VMA or VMA + 250 µM $CuSO_4$ was tracked over time for strains ISU-4956 ($rfk\text{-}1^{TAG>TGG}$) and ISU-4957 ($rfk\text{-}1^{Sk\text{-}2}$). Complete growth assay results are provided in Table 2.

Figure 4 $RSK^{Sk\text{-}2}$ neutralizes $RFK\text{-}1^{B}$. **(**A) The relative positions of *N. crassa* genes *ncu03754*, *ccg-1*, and *ncu03752* on chromosome V are illustrated at the top the panel. Coding directions and coding sequences are depicted as black arrows and white rectangles, respectively. Intron positions are not indicated. The diagram was drawn to scale. Only part of the *ncu03754* coding sequence is represented in the diagram. The orange bar represents the 354 bp of DNA that were deleted and replaced with *rsk* coding sequences and a selectable marker (*hph*). (B) Images of *N. crassa* cultures after five days of growth. Conidial suspensions were inoculated to the center of 100 mm culture dishes containing VMA or VMA + 250 µM $CuSO_4$. The images for ISU-4956 are identical to those shown in Figure 3B. (C) Linear growth on VMA was tracked over time for strains ISU-4956 ($rfk\text{-}1^{TAG>TGG}$), ISU-4962 ($rfk\text{-}1^{TAG>TGG}$ $rsk^{Sk\text{-}2}$), and ISU-3866 (wild type). Complete growth assay results are provided in Table 2.

Figure S1 Construction of $rsk^{Sk\text{-}2}$*-hph* DNA fragment**.** **(**A) The relative positions of *N. crassa* genes *ncu09153*, *ncu09152,* and *rsk* on chromosome III in *Sk-2* strain FGSC 7426 (Svedberg *et al.* 2018) are shown. A putative start codon for *ncu09152* was not identified (indicated by the jagged side of the *ncu09152* white rectangle). The diagram was drawn to scale and the orange

bar represents the 362 bp of DNA that were deleted and replaced with a selectable marker (*hph*). Most of the approximately 6800 bp of DNA sequence depicted to the right of *rsk* in the diagram has a low GC content, which possibly explains our inability to identify a protein coding gene in this region.

Figure S2 Sequence and features of AH36 from *Sk-2*. AH36 was defined by Rhoades *et al.* (2019) as a 1481 bp *rfk-1*-spanning interval of *Sk-2* DNA (GenBank KJ908288.1: positions 27900–29380). The sequence of AH36 is shown. The *rfk-1* start codon is highlighted in green. Intronic sequences are highlighted in gray. The first (TAG) and second (TAA) stop codons are highlighted in red. The first stop codon was changed to TAA in the *rfk-1*$^{TAG>TAA}$ allele and to TGG in the *rfk-1*$^{TAG>TGG}$ allele.

Figure 1

RFK-1[A]

MACPTGFFTALFGKLLTIPIWVLVFVFNALFVFPRFWV
WRLPPRLQHEQQQQDRNDDEWQRQQQDRRVVVWHPPPP
PDVEMALQDNPTAAPAEPADLDHPAP

RFK-1[B]

MACPTGFFTALFGKLLTIPIWVLVFVFNALFVFPRFWV
WRLPPRLQHEQQQQDRNDDEWQRQQQDRRVVVWHPPPP
PDVEMALQDNPTAAPAEPADLDHPAPWWRRWVADDAYP
AVHFCVTAANAVTQGL

Figure 2

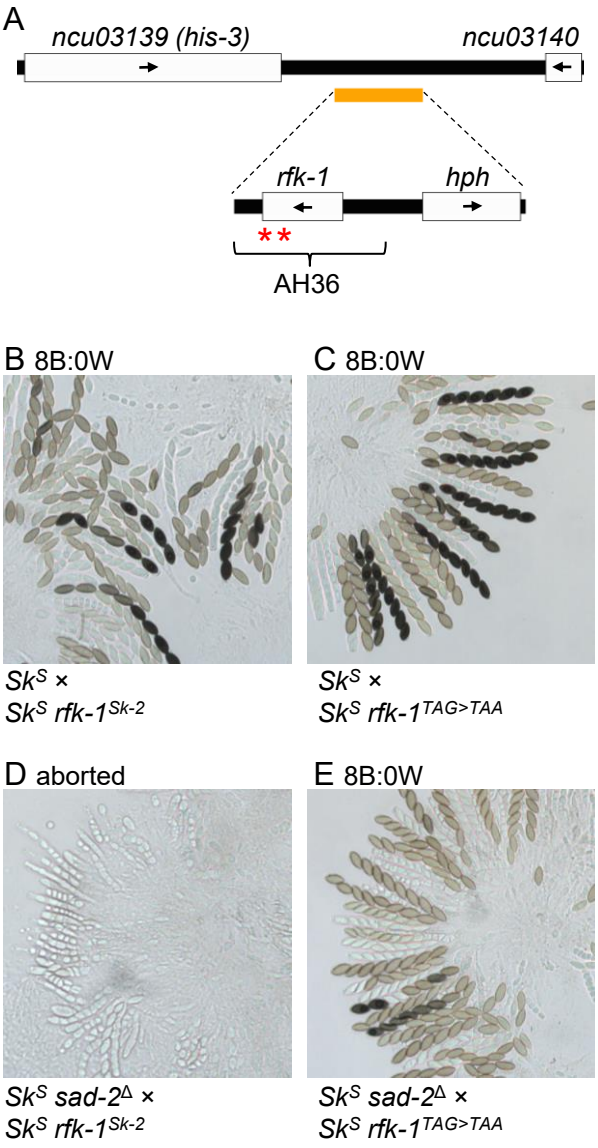

Figure 3

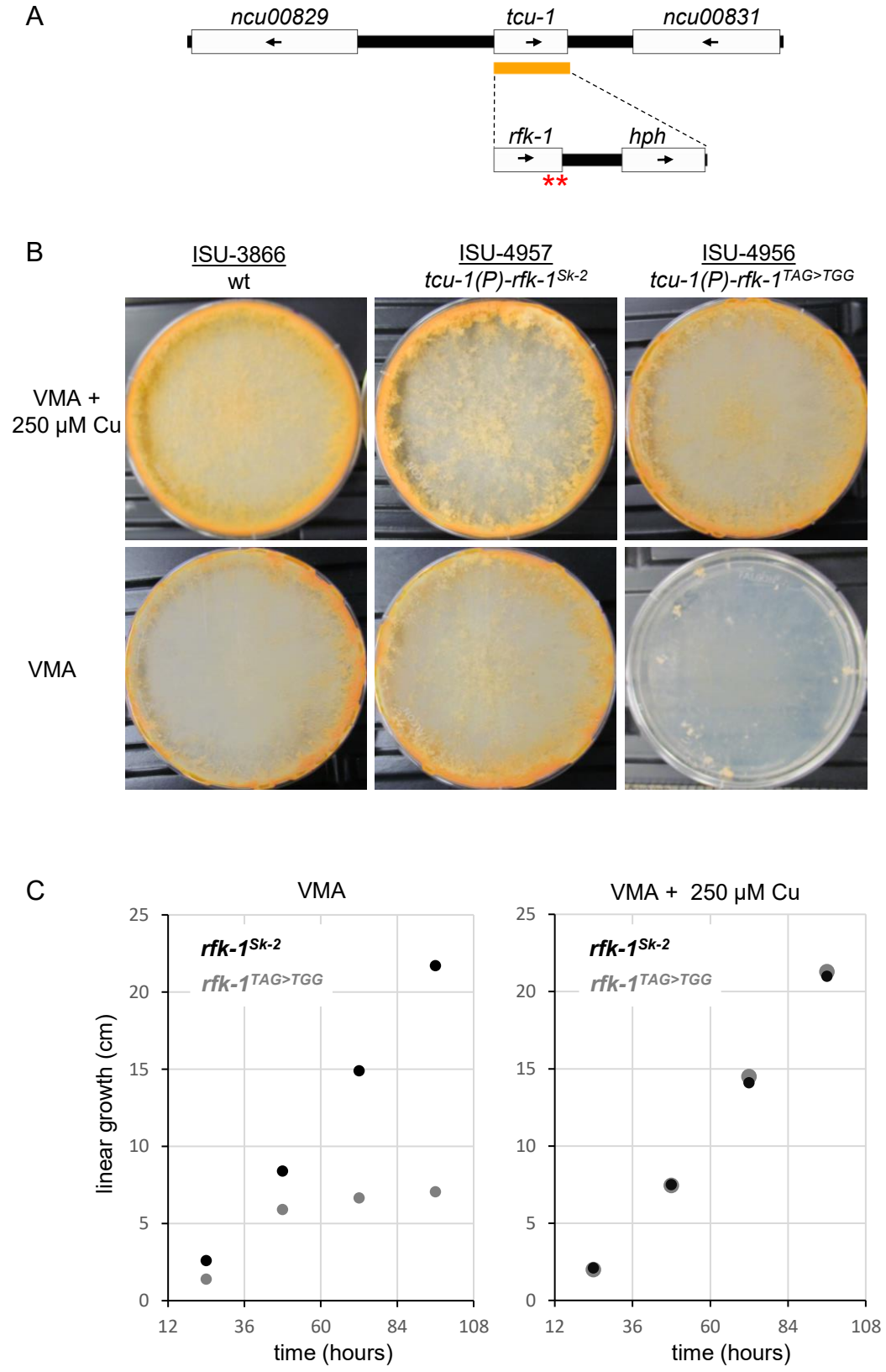

Figure 4

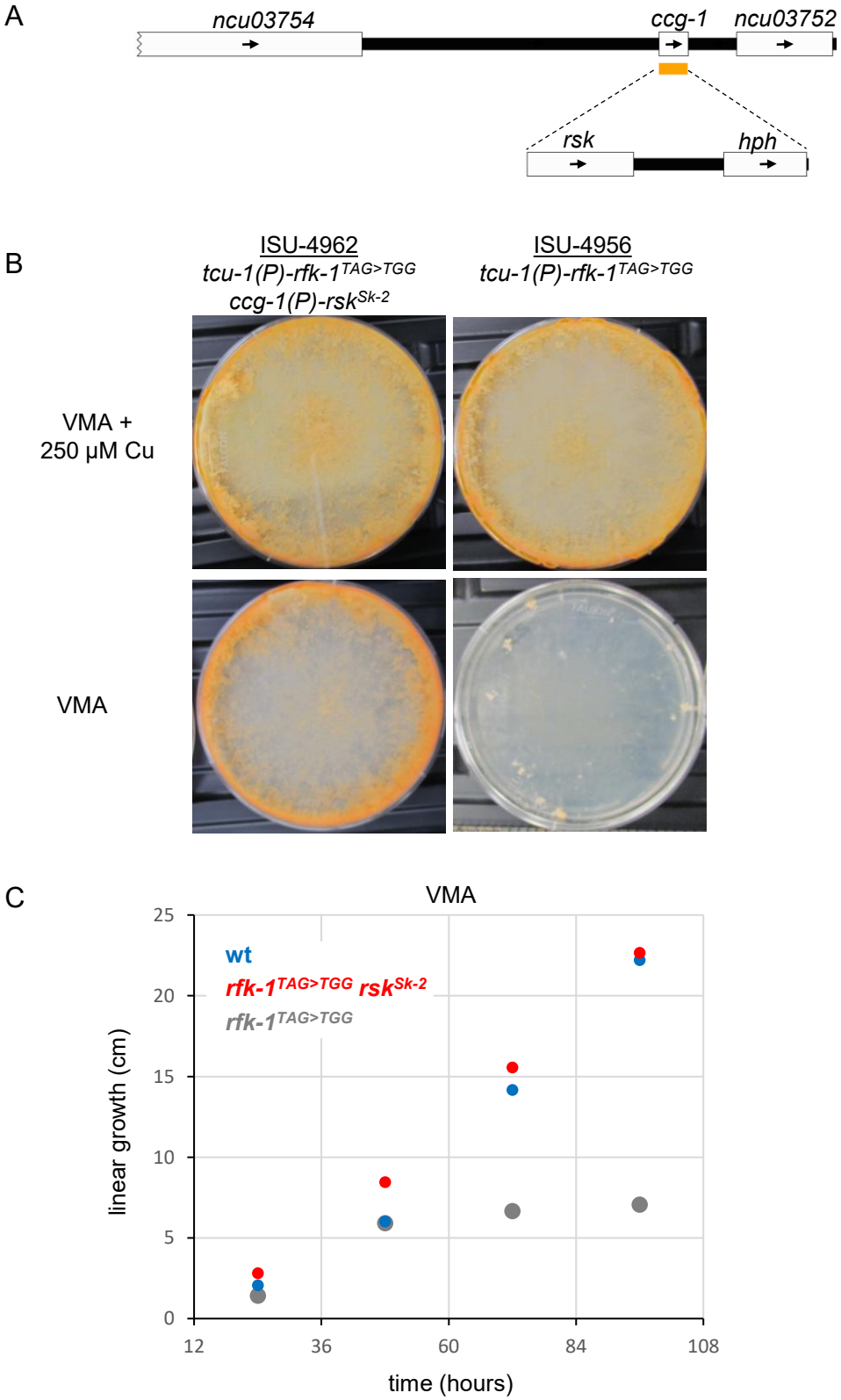

Figure S1

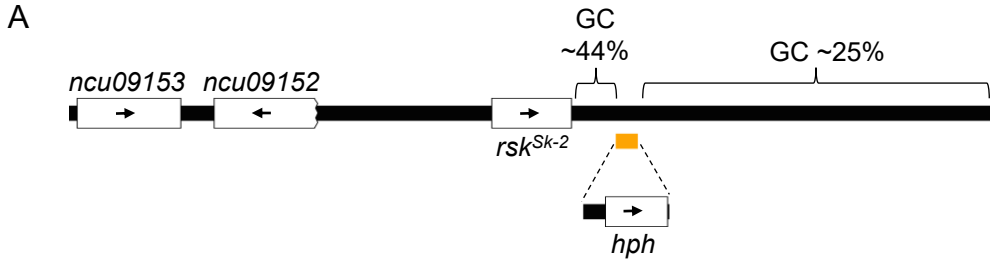

Figure S2

CATTGATACCGAGTCTTTCCGTTCTTAAGGTTGGAGTGAGGATATGATCCGGCACGTCGAAGGAGGAACTA
TGGTAAATAAGTCAGTCATCATCAAGGAAAAGAACAGTATTAGGTGCCTTCAAGTTACCTACCTTCTCCGA
CGGGGGCCCTGCCTTCCCTTAGTTCTCTCATGAAGCTGGAAGTTATATCCTAACCCACTACTGACAAAACA
AAGCAAGAGCTGCTGCCCCAACTATAGACAGCACGCTTTTCCACCTCAGTTGGGGCACCTAGAAAGCTATA
AGATCCCTCTTCCCCCGGCCCAACCTCTCCTCAGAATTTCTTTTTTTCTCCAACATTGTTAAGAACTTTGT
TTTTGGAAAATGGCCTGCCCCACAGGGTTTTTTACCGCTCTTTTTGGCAAACTCCTCACCATCCCCATTTG
GGTGTTGGTGTTTGTATTCAATGCTCTGTTTGTCTTCCCCCGGTTTTGGGTCTGGTAAGTCTCCTTCATGT
TCCAATTCATTTTTGTTTTTTCCTTTCTCTTCTCGTCTCCTTCATGTTCCAATTCATTTTTGTTTTTTTCC
TTTCTCTTCTCGTCTCCTTCATGTTCCAGTTCATTTTTGTTTTTTCCTTTCTCTTCTCGTCTCCTTCATGT
TCCAATTCATTTTTGTTTTTTTCCTTTCTCTTCTCGTCTCCTTCATGTTCCAGTTCATTTTTGTTTTTTCC
TTTCTCTTCTCGTCTCCTTCATGTTCCAATTCATTTTTGTTTTTTTCCTTTCTCTTCTCGTCTCCTTCATG
TTCCAATTCATTTTTTTTTGTCCTTTCTCTTCTCGTCTCCTTACAGTTTACCTTATCCTCTCGGTCCTCTC
TGTCTTTCGCTAACCAGGAACAGGCGCTTACCACCACGGCTGCAACACGAGCAGCAGCAGCAGGACCGGAA
CGATGACGAATGGCAGCGGCAGCAACAGGACAGGCGGGTTGTGGTTTGGCACCCACCGCCCCCTCCAGACG
TGGAGATGGCCCTCCAAGACAATCCCACTGCCGCCCCCGCAGAGCCGGCTGACCTCGACCACCCAGCGCCG
TAGTGGCGGCGCTGGGTGGCCGACGAGTAGGTCAATGCTATTCCCAGATTATGAAATGTATCGCTGACAGT
TGCACACCAGTGCCTACCCGGCCGTCCACTTCTGCGTGACCGCAGCCAATGCGGTCACGCAGGGGTTGTAA
TTCCACGTGAGCATTCCCCACCTTCTCTCGGGACCGACTTCCGTATCAACCCCAAATTTATCGGACTGACC
CGTCCGAATCAAGGCGAACCGAGAGGACACAGACAAGGCCCACGTCCGCCATCAGCATTCCCAGCTGGCCG
ACCGCACCGCCGCAACTCCCACTTTACCTCAACACCAGAATACGGAATCGGTACATCGACAGCAGCATCAT
CATCATCAATATCACCACCTCCACTTGGCGCGCACTTGCGGAAAACGTCCCGCTACACCGT C

Table 1 Strains used in this study

Strain name (alias)	Genotype
F2-23 (RTH1005.1)	*rid; fl A*
F2-26 (RTH1005.2)	*rid; fl a*
FGSC 10340 (RZS27.10)	*rid; mus-51^{RIP70} a*
ISU-3037 (RTH1623.2)	*rid; fl; sad-2$^{\Delta}$::hph a*
ISU-3866 (RAB1.8)	*rid A*
ISU-4954 (HNR218.2.1)	*rid his-3^{+}::rfk-1^{Sk-2}-hph; mus-52$^{\Delta}$::bar A*
ISU-4955 (HNR220.1.1)	*rid his-3^{+}::rfk-1$^{TAG>TAA}$-hph; mus-52$^{\Delta}$::bar A*
ISU-4956 (CNR236.1.1)	*rid tcu-1$^{\Delta}$::tcu-1(P)-rfk-1$^{TAG>TGG}$-hph; mus-51^{RIP70} a*
ISU-4957 (CNR238.1.1)	*rid tcu-1$^{\Delta}$::tcu-1(P)-rfk-1^{Sk-2}-hph; mus-51^{RIP70} a*
ISU-4958 (TNR278.1)	*rid; Sk-2 rsk^{Sk-2}-hph; mus-51$^{\Delta}$::bar A*
ISU-4959 (TNR281.4)	*rid; mus-51^{RIP70}; ccg-1$^{\Delta}$::ccg-1(P)-rsk^{Sk-2} a*
ISU-4961 (RNR281.4.2)	*rid; mus-5^{RIP70}; ccg-1$^{\Delta}$::ccg-1(P)-rsk^{Sk-2} A*
ISU-4962 (RNR301.2)	*rid tcu-1$^{\Delta}$::tcu-1(P)-rfk-1$^{TAG>TGG}$-hph; mus-51?; ccg-1$^{\Delta}$::ccg-1(P)-rsk^{Sk-2}-hph a*
ISU-4963 (RNR302.1)	*rid tcu-1$^{\Delta}$::tcu-1(P)-rfk-1^{Sk-2}-hph; mus-51?; ccg-1$^{\Delta}$::ccg-1(P)-rsk^{Sk-2}-hph a*
P8-42	*rid his-3; mus-51$^{\Delta}$::bar a*
P8-43	*rid his-3; mus-52$^{\Delta}$::bar A*
P15-53 (RTH1122.22)	*rid; Sk-2; mus-51$^{\Delta}$::bar A*

Strain derivations
ISU-4958 is a heterokaryotic transformant pf P15-53.
ISU-4959 is a heterokaryotic transformant of FGSC 10340.
ISU-4961 is an offspring from a cross between ISU-4959 and F2-23.
ISU-4962 is an offspring from a cross between ISU-4956 and ISU-4961. A unidirectional cross was performed on standard SCA with ISU-4961 as female.
ISU-4963 is an offspring from a cross between ISU-4957 and ISU-4961. A unidirectional cross was performed on standard SCA with ISU-4961 as female.

Table 2 Average linear growth rates in centimeters per hour

Strain and time interval	*tcu-1(P)-rfk-1*	*ccg-1(P)-rsk*$^{Sk-2}$	VMA	VMA + 250 µM Cu
24-48 h				
A	no	no	0.165 ± 0.003	0.192 ± 0.006
B	yes (TAG>TGG)	no	0.188 ± 0.012	0.227 ± 0.021
C	yes (*Sk-2*)	no	0.242 ± 0.012	0.225 ± 0.000
D	yes (TAG>TGG)	yes	0.235 ± 0.003	0.235 ± 0.009
E	yes (*Sk-2*)	yes	0.242 ± 0.018	0.242 ± 0.000
48-72 h				
A	no	no	0.340 ± 0.009	0.300 ± 0.006
B	yes (TAG>TGG)	no	0.031 ± 0.003	0.294 ± 0.003
C	yes (*Sk-2*)	no	0.271 ± 0.018	0.275 ± 0.012
D	yes (TAG>TGG)	yes	0.296 ± 0.012	0.308 ± 0.000
E	yes (*Sk-2*)	yes	0.306 ± 0.003	0.304 ± 0.006
72-96 h				
A	no	no	0.335 ± 0.009	0.340 ± 0.015
B	yes (TAG>TGG)	no	0.017 ± 0.000	0.283 ± 0.000
C	yes (*Sk-2*)	no	0.283 ± 0.012	0.288 ± 0.012
D	yes (TAG>TGG)	yes	0.296 ± 0.006	0.269 ± 0.015
E	yes (*Sk-2*)	yes	0.300 ± 0.000	0.296 ± 0.006

The presence of *tcu-1(P)-rfk-1*$^{Sk-2}$, *tcu-1(P)-rfk-1*$^{TAG>TAA,}$ and *ccg-1(P)-rsk*$^{Sk-2}$ alleles in each strain is indicated in columns 2 and 3. Strains are as follows: A, ISU-3866; B, ISU-4956; C, ISU-4957; D, ISU-4962; E, ISU-4963. Raw data is provided in Table S2.

Table S1 Primers used in this study

Name	Sequence (5 > 3)
12	AACTGATATTGAAGGAGCATTTTTTGG
13	AACTGGTTCCCGGTCGGCAT
353	TTTTGCGGCCGCCATTGATACCGAGTCTTTCCGTTC
639	AAAAGCGGCCGCGACGGTGTAGCGGGACGTTTTCC
1727	CACGGCGCTGGGTGGTCGAGGTC
1728	GTGGCGGCGCTGGGTGGCCGACGAGTAGGTCAATGCTATT
1789	TGGCGGCGCTGGGTGGCCGACGAGTAGGTCAATGCTATTC
1791	TTACGGCGCTGGGTGGTCGAGGTC
1843	ATGGCCTGCCCCACAGGGTT
1844	AACTGGTTCCCGGTCGGCAT
1845	TCCCTGGTTGCTGACTCCTTGTC
1846	GGTAAAAAACCCTGTGGGGCAGGCCATGGTTGGTTGGGGATGTGTgtg
1847	AGTAGATGCCGACCGGGAACCAGTTAGGATGGAAGAAGGGACGGAAGA
1848	CCGCGCTATCGACCTCAACTACA
1849	GCTCATATTCCAGGCGAACGACA
1850	GTGCAGGCTTGGCTTCAGGACTT
1985	GCGGTCGAAAGTGTATGCCAAAT
1986	AAAAAATGCTCCTTCAATATCAGTTAGAAGGGTTGGGAGGGTGCTG
1987	GAGTAGATGCCGACCGGGAACCAGTTCTAGGTCTACGCCGCTTTCAATCTT
1988	TCGCCGCCTTCCTAATCTAAATAGC
1989	CGGCTTCATTTGAGATCGAGGTTTT
1990	CTCTATTGCCCAGTGGCTAGTGCTC
1997	ATGTTATCATCCTTCGTCCGGACCC
1998	AACTGGTTCCCGGTCGGCAT
2011	AAGGAGCAGTCCATCTGCGTGAA
2012	CGACGGGTCCGGACGAAGGATGATAACATTTTGGTTGATGTGAGGGGTTGTG
2013	GAGTAGATGCCGACCGGGAACCAGTTTGCTACCCACTAAGCGACTTTACCA
2014	TACCAAATCAACCCCAGCCCATC
2015	CAAAGCCACATCACTGGGCACTT
2016	TCAGCCTTGGCATAAACCATCCA

Table S2 Linear growth measurements of various strains on VMA and VMA + 250 µM Cu

		VMA			VMA + 250 µM Cu		
	Hours	Rep A	Rep B	Avg ± STDEV (cm)	Rep A	Rep B	Avg ± STDEV (cm)
ISU-3866	24	2.1	2	2.05 ± 0.07	2.4	2.2	2.3 ± 0.14
	48	6.1	5.9	6 ± 0.14	7.1	6.7	6.9 ± 0.28
	72	14.4	13.9	14.15 ± 0.35	14.4	13.8	14.1 ± 0.42
	96	22.6	21.8	22.2 ± 0.57	22.8	21.7	22.25 ± 0.78
	120	27	27	27 ± 0.00	27	27	27 ± 0.00
	144	27	27	27 ± 0.00	27	27	27 ± 0.00
	168	27	27	27 ± 0.00	27	27	27 ± 0.00
ISU-4956	24	1.3	1.5	1.4 ± 0.14	2	2	2 ± 0.00
	48	6	5.8	5.9 ± 0.14	7.1	7.8	7.45 ± 0.49
	72	6.7	6.6	6.65 ± 0.07	14.2	14.8	14.5 ± 0.42
	96	7.1	7	7.05 ± 0.07	21	21.6	21.3 ± 0.42
	120	7.1	7	7.05 ± 0.07	27	27	27 ± 0.00
	144	7.1	7	7.05 ± 0.07	27	27	27 ± 0.00
	168	7.1	7	7.05 ± 0.07	27	27	27 ± 0.00
ISU-4957	24	2.7	2.5	2.6 ± 0.14	2.1	2.1	2.1 ± 0.00
	48	8.7	8.1	8.4 ± 0.42	7.5	7.5	7.5 ± 0.00
	72	15.5	14.3	14.9 ± 0.85	14.3	13.9	14.1 ± 0.28
	96	22.5	20.9	21.7 ± 1.13	21.4	20.6	21 ± 0.57
	120	27	27	27 ± 0.00	27	27	27 ± 0.00
	144	27	27	27 ± 0.00	27	27	27 ± 0.00
	168	27	27	27 ± 0.00	27	27	27 ± 0.00
ISU-4962	24	3	2.6	2.8 ± 0.28	2.5	2.7	2.6 ± 0.14
	48	8.7	8.2	8.45 ± 0.35	8	8.5	8.25 ± 0.35
	72	16	15.1	15.55 ± 0.64	15.4	15.9	15.65 ± 0.35
	96	23.2	22.1	22.65 ± 0.78	22.1	22.1	22.1 ± 0.00
	120	27	27	27 ± 0.00	27	27	27 ± 0.00
	144	27	27	27 ± 0.00	27	27	27 ± 0.00
	168	27	27	27 ± 0.00	27	27	27 ± 0.00
ISU-4963	24	2.4	2.4	2.4 ± 0.00	2.7	2.6	2.65 ± 0.07
	48	7.9	8.5	8.2 ± 0.42	8.5	8.4	8.45 ± 0.07
	72	15.3	15.8	15.55 ± 0.35	15.7	15.8	15.75 ± 0.07
	96	22.5	23	22.75 ± 0.35	22.9	22.8	22.85 ± 0.07
	120	27	27	27 ± 0.00	27	27	27 ± 0.00
	144	27	27	27 ± 0.00	27	27	27 ± 0.00
	168	27	27	27 ± 0.00	27	27	27 ± 0.00

Two replicate growth tubes were inoculated for each strain per medium type. The maximum distance that could be traveled by each strain is approximately 27 cm due to constraints set by the length of the serological pipettes used as growth tubes for this experiment (see methods).